Journal of Materials Science and Engineering with Advanced Technology
Volume 2, Number 2, 2010, Pages 113-134

FABRICATION AND CHARACTERIZATION OF ELECTROSPUN CHITOSAN/POLY(L-LACTIC ACID) NANO/MICRO FIBERS AS A SCAFFOLD FOR BONE REGENERATION

XUXU BAO, AKIRA TERAMOTO and KOJI ABE

Department of Functional Polymer Science
Faculty of Textile Science and Technology
Shinshu University
Ueda, Nagano
Japan
e-mail: baqiaobaoxu@hotmail.com

Abstract

Bone is a natural composite mainly made from nano/micro-fibers of collagen and hydroxyapatite. In tissue-engineered bone regeneration, it is important to synthesize nano-composite scaffolds with good biocompatibility, high bioactivity, and strong bonding properties. In this study, a chitosan/poly(L-lactic acid) (CS/PLLA) blend of nano/micro fibers were prepared by using electrospinning, to form a three-dimensional porous scaffold for bone regeneration. FT-IR and tensile tests show that we succeed in fabricating CS/PLLA blend fibers with enhanced tensile properties, while maintaining the bioactive amino groups. Moreover, water contact angle and water uptake results show that chitosan content increases the hydrophilicity of the fibrous scaffold, which has positive effects on osteoblast adhesion. In cell proliferation, differentiation and mineralization assays using mice osteoblast-like (MC3T3-E1) cells, the CS/PLLA blends of 1:1 and 2:1 had almost identical bioactivities and were the most promising for bone regeneration.

Keywords and phrases: chitosan, PLLA, scaffold, osteoblast-like, electrospinning.

Received September 28, 2010

1. Introduction

Tissue engineering is an emerging multidisciplinary field that aims to restore, maintain or enhance tissue and organ regeneration. To guide the transition of tissue engineering from a cellular to tissue level, we will use a three-dimensional (3D) scaffold to act as a synthetic extracellular matrix (ECM). This will help to promote the organization of cells in a 3D architecture and direct the growth and formation of the desired tissue [7, 16, 22]. Bone repair has being researched widely in tissue engineering; as bone has limited capacity for self-repair due to the low rate of mitosis in chondrocytes and poor vascular supply [7, 13, 22]. It has been recognized that certain ceramics, such as bioglass, sintered hydroxyapatite, and sintered β-tricalcium phosphate [4], have been used as artificial implants for bone defects. They have been shown to spontaneously bond to living bone without the formation of surrounding fibrous tissue. However, a number of problems have been encountered with the use of these materials due to the release of acidic degradation products that lead to inflammatory responses. To address these limitations, new porous biodegradable materials, with osteoconductive properties, need to be developed for bone tissue engineering [5, 12, 20, 21, 24].

Chitosan, a linear polysaccharide composed of randomly distributed β-(1-4)-linked D-glucosamine (deacetylated) and N-acetyl-D-glucosamine (acetylated) units, has already been successfully used for drug delivery, sutures, and skin repair. One of the most exceptional features of chitosan is how easily it can be processed into porous scaffolds for cell transplantation and tissue regeneration. Nevertheless, the poor mechanical strength of chitosan limits its application in bone tissue engineering [5, 12, 15]. One strategy that we were interested in was to combine chitosan with a synthetic polyester, such as poly-L-lactide (PLLA), which is also being evaluated as a biodegradable material for tissue engineering. However, a major drawback of PLLA is that, it can elicit undesirable inflammatory and allergenic reactions as it decreases the local pH via its hydrolytic degradation. The discovery of an optimal combination of chitosan and PLLA may overcome some of the drawbacks of the polymers alone, thereby producing a composite material with potentially beneficial characteristics for biomedical applications.

Many studies have been devoted to the crosslinking of chitosan with PLLA producing composite materials with strong mechanical properties [1, 2, 6, 10]. Crosslinking of chitosan and PLLA by 1-(3-Dimethylaminopropyl)-3-ethylcarbodiimide hydrochloride (EDC), a carbodiimide crosslinker, forms a covalent bond between the amino groups in chitosan and the carboxyl groups in chitosan. However, as the N-acetylglucosamine moiety in chitosan is active in specific interactions with certain proteins, growth factors and their receptors, the use of EDC as a crosslinker may decrease the bioactivity of chitosan. Therefore, to retain the bioactivity of chitosan, we blended PLLA with chitosan by using a trifluoroacetic acid-HFIP solution system, without crosslinking.

Electrospinning is a simple and effective technique that allows us to obtain ultra-fine fibers, with diameters ranging from a few nanometers to micrometers. The electrospun mats are particularly suitable for biomedical applications [8, 11, 18, 27], as they can mimic the extracellular matrix (ECM), thereby enhancing cellular migration and proliferation.

To determine the optimal blend ratio, CS/PLLA nanofibers of different blends were prepared via electrospinning. Degradation, hydrophilicity, and biocompatibility of the CS/PLLA fibrous scaffolds were evaluated. A model commonly used to study osteogenic growth is the MC3T3-E1 osteoblast-like cell line, which is characterized by distinct proliferation and differentiation properties. It reproduces a temporal programmer consistent with the osteoblast differentiation that occurs during bone formation *in vitro* [3, 9].

2. Materials and Methods

2.1. Materials

Poly(L-lactic acid) ($\mathrm{Mn} = 1 \times 10^4 - 2.2 \times 10^4$) was purchased from Toyota Eco Plastic U'z (Japan). Chitosan (CS) (100 DVL; $\mathrm{Mn} = 4.6 \times 10^4 - 8.3 \times 10^4$, degree of deacetylation ~85%) was purchased from Dainichiseka Color and Chemicals Mfg. Co. Ltd., (Japan).

2.2. Preparation of fibrous scaffolds

PLLA was dissolved in 1, 1, 13, 3, 3-hexafluoro-2-propanol (HFIP; Wako, Japan) with a concentration of 10% (w/v). Chitosan was dissolved in the trifluoroacetic acid with a concentration of 10% (w/v), at room temperature. The electrospinning solutions were prepared by mixing PLLA and chitosan solutions with the following weight ratios: 1:0, 2:1, 1:1, 1:2, and 0:1, respectively. Nano/micro fibers were prepared via electrospinning (Nanofiber Electrospinning Units, Kato TECH Co., Japan). Samples were washed with 1N NaOH, followed by vacuum-drying for 24 hours to remove residue solvents. All samples were washed with deionized water and dried at 30˚C prior to characterization.

2.3. Characterization of scaffolds

2.3.1. SEM observation

Samples were cut into pieces of appropriate size, fixed on the sample plant and coated with gold and palladium for 90s using a sputter coater (Hitachi, Japan). The porous morphologies of the scaffolds were examined by SEM (S-2380N, Hitachi, Japan).

2.3.2. FT-IR

FT-IR spectra were recorded on a Smiths DuraSampI IR-II IRPrestige-21, with 16 scans per sample ranging from 4000 to 800 cm^{-1}, at a resolution of 4cm^{-1}.

2.3.3. Water contact angle and water uptake test

To investigate the hydrophilicity of the scaffold surfaces, the contact angles were measured by using the sessile drop method and drop shape analysis system at 20˚C ($n = 5$).

Samples ($1cm \times 5cm$) were placed into 20ml of deionized water at room temperature for 1 hour; the swollen samples were then weighted after removing excess surface water by using filter paper. Water uptake of each sample was calculated ($n = 5$) as follows:

$$\text{Water uptake } (\%) = (W_s - W_d)/W_d \times 100,$$

where W_s is the weight of the swollen scaffold and W_d is the weight of the dry scaffold.

2.3.4. Tensile test

Mechanical properties, in terms of the stress and elongation at breaking point of the fibers, were measured according to the ISO 2062:1993(E) standard test method, using a universal testing machine (ORIENTEC Ltd. Co. Japan). The load cell, the gauge length, and the strain rate were 10N, 50mm, and 1mm/min, respectively. The electrospun mats with an initial size of 80mm (length) × 50mm (width) were preconditioned at room temperature and 55% humidity for 24 hours. During the measurements, both the ambient temperature and the relative humidity were recorded (20 ± 2°C and 55 ± 5%). The stress and the elongation at the breaking point were recorded ($n = 5$).

2.3.5. Degradation test

The remaining weight of samples were measured in pH 7.4 lysozyme (0.05wt%), in PBS solution at 37˚C. During degradation, the samples (initial weight: W_0) were removed from the degradation medium at specific time intervals and washed with deionized water. Following this, the samples were dried in a vacuum to remove all the residual medium liquids, and subsequently weighed (W). Weight remaining ratio was calculated by using the following equation ($n = 5$):

$$\text{Weight remaining ratio } (\%) = W/W_0 \times 100.$$

2.3.6. Cell culture

MC3T3-E1 cells, an immortalized cell line derived from mouse calvarial tissue, were obtained from the RIKEN Cell Bank (Tsukuba, Japan) and cultured in α-modified minimal essential medium (α-MEM; GIBCO). The medium contained 10% heat-inactivated fetal bovine serum (FBS, GIBCO), 100U/ml penicilline and 100U/ml streptomycin. All *in vitro* cell incubations were performed in a HITACHI incubator (Japan) at 37˚C, in a 5% CO_2 atmosphere with 100% relative humidity. Culture medium was refreshed every 2 days. Cells cultured on tissue culture dishes (TCD) were evaluated as controls. TCDs were composed of optically

clear, high-grade polystyrene Nunc™ dishes, prepared by using a vacuum-gas plasma sterilization treatment. The incorporation of nitrogen-containing cations on the surface of the dishes has been correlated with the attachment and spreading of primary endothelial cells in a clonal cell-growth assay [23].

2.3.7. Cell adhesion ratio

Electrospun fibrous mats were cut into pieces with a size of $1.5\text{cm} \times 1.5\text{cm}$ and placed in a 12-well TCD. Cells were seeded $(2.5 \times 10^4 \text{cells/well})$ on the scaffolds and cultured under the conditions described in Subsection 2.3.6. The cells were allowed to attach to the scaffolds in a humidified incubator $(37°\text{C}, 5\%\ CO_2)$ for 1, 3, 6, and 24 hours. At each time interval, unattached cells were collected by thoroughly washing with PBS and counted under a microscope (N). The adhesion ratio was calculated by using the following equation (n = 3):

$$\text{Adhesion ratio } (\%) = (1 - N/2.5 \times 10^4) \times 100.$$

2.3.8. Proliferation assays

For proliferation assays, 1×10^5 cells/well were seeded in 1ml of culture medium supplemented with 0.1% β-glycerophosphate. At specific time periods during a 14-days cultivation period, 10μL of Tetra Color ONE (Seikagaku Corporation, Tokyo, Japan) reagent, containing tetrazolium monosodium salt, was added to each well and cells were incubated for an additional 2 hours. Absorbance at 450nm was measured with the Biotrak II plate reader (GE, U.S.). The data reported were the mean of three examinations.

2.3.9. Immunohistochemical staining

Using the same seeding conditions as in Subsection 2.3.8, cells were cultivated for 3 days, following which samples for cytoskeletal staining were fixed with acetone for 40min at –20°C and subsequently washed twice with PBS. Samples were blocked with 10% FBS for 30 minutes, to reduce non-specific background staining. Immunostaining for vinculin was performed by using a monoclonal mouse anti-vinculin IgG1 primary

antibody (1:400 dilution; Sigma-Aldrich, USA) and a goat anti-rabbit IgG (H+L) Alexa Fluor 568-conjugated secondary antibody (1:800 dilution; Molecular Probes Europe BV, The Netherlands). Finally, cells were mounted for 1 hour at room temperature, using a DAPI (4', 6-diamidino-2-phenylindole, Dojindo Molecular Technologies, Japan) nuclear stain. Staining was visualized by using a Zeiss Axio Imager M1 fluorescence microscope equipped with AxioCam MRm. Alexa-568 produces red fluorescence at 568nm and DAPI produces blue fluorescence at 345nm.

2.3.10. ALP activity

The levels of cell differentiation on these scaffolds were assessed by determining the level of alkaline phosphatase (ALP) activity. Cells were seeded and cultured as described in Subsection 2.3.8. ALP activity was measured at specific time periods over 14 days of cultivation. 500μL β-nitrophenylphosphate solution, containing 1m mol/l $MgCl_2$ (Sigma, USA), was add to the culture medium and incubated for 10min at 37°C. The enzymatic reaction was stopped by adding 500μL of 0.2N NaOH, following which the absorbance at 405nm was measured by using a Biotrak II plate reader. The data reported were the mean of three examinations.

2.3.11. Calcium deposition

Cells were seeded and cultured as described in Subsection 2.3.8. Calcium deposition was measured at specific time periods during 14 days of cultivation. Cells were washed twice in PBS and incubated for 2 hours in 1N HCl. The calcium deposit in each solution was then measured by using a calcium C test kit (Wako, Japan). The data reported were the mean of three examinations.

3. Results and Discussion

To mimic the 3D structure of natural ECM (i.e., the nano/micro scale fibrous network of collagens and proteoglycans that promotes the attachment, proliferation, and differentiation of cells), we employed electrospinning as a proven, novel and effective method of producing such fibrous structures [15].

Figure 1 shows the SEM images (1) and fiber diameter distribution (2) of CS/PLLA fibers with weight ratios of 1:0, 2:1, 1:1, 1:2, and 1:0. In all cases, the fibers were randomly oriented on the substrate, without any evidence of beads-on-string morphology. All fibers exhibited a smooth surface, with average diameters ranging from 800nm to 1100nm, and no remarkable structural differences between them. Scaffolds showed a homogeneous porous structure with pore sizes ranging from 153μm to 293μm.

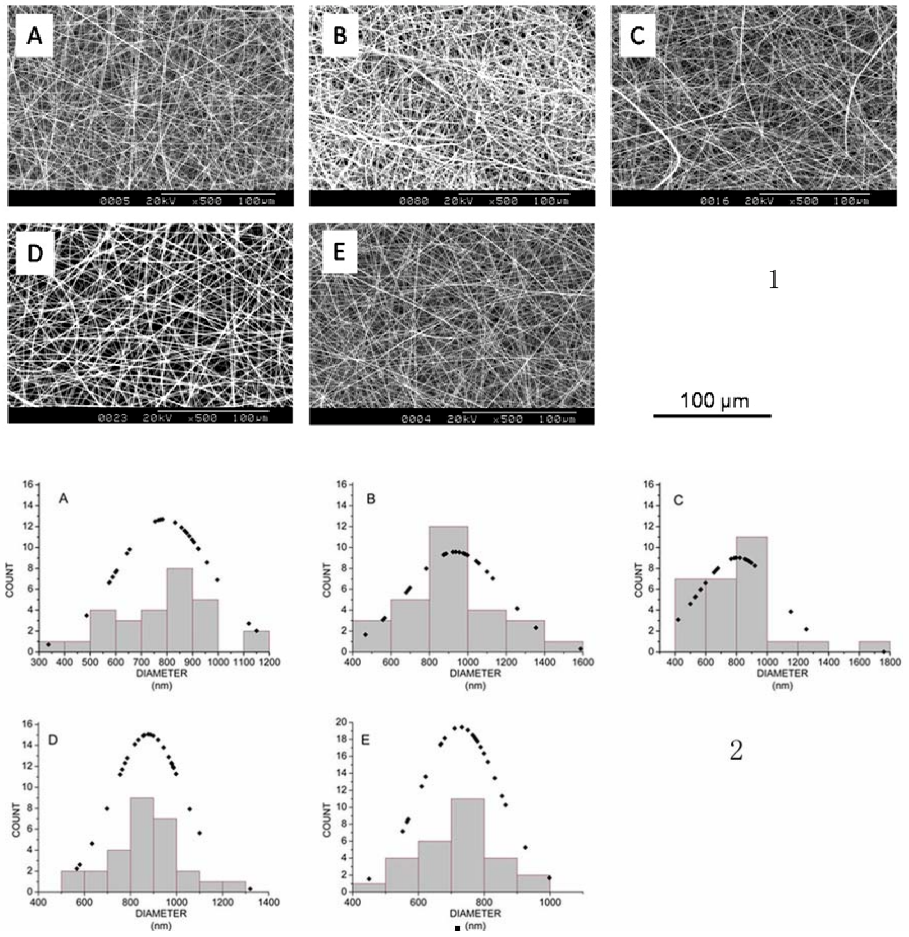

Figure 1. Scanning electronic microscopy images (1) and fiber diameter distributions (2) of each scaffold: (A) CS/PLLA = 2:1; (B) CS; (C) CS/PLLA = 1:1; (D) CS/PLLA = 2:1; (E) PLLA.

To confirm the chemical structural changes, CS/PLLA scaffolds with different compositions were investigated by IR spectroscopy (Figure 2). Chitosan fibers displayed characteristic absorption bands at 1660cm^{-1} and 1540cm^{-1}, representing the amide I and II characteristic absorption bands, respectively. PLLA fibers depicted characteristic absorption bands at 1759, 1185, 1130, and 1089cm^{-1}, representing the backbone ester group of PLLA. For blend scaffolds the peak positions of amide I and II were almost unchanged. This may be explained by a weak molecular interaction between chitosan and PLLA, owing to PLLA having too few −OH groups to form hydrogen bonds with the −OH and $-NH_2$ groups in chitosan.

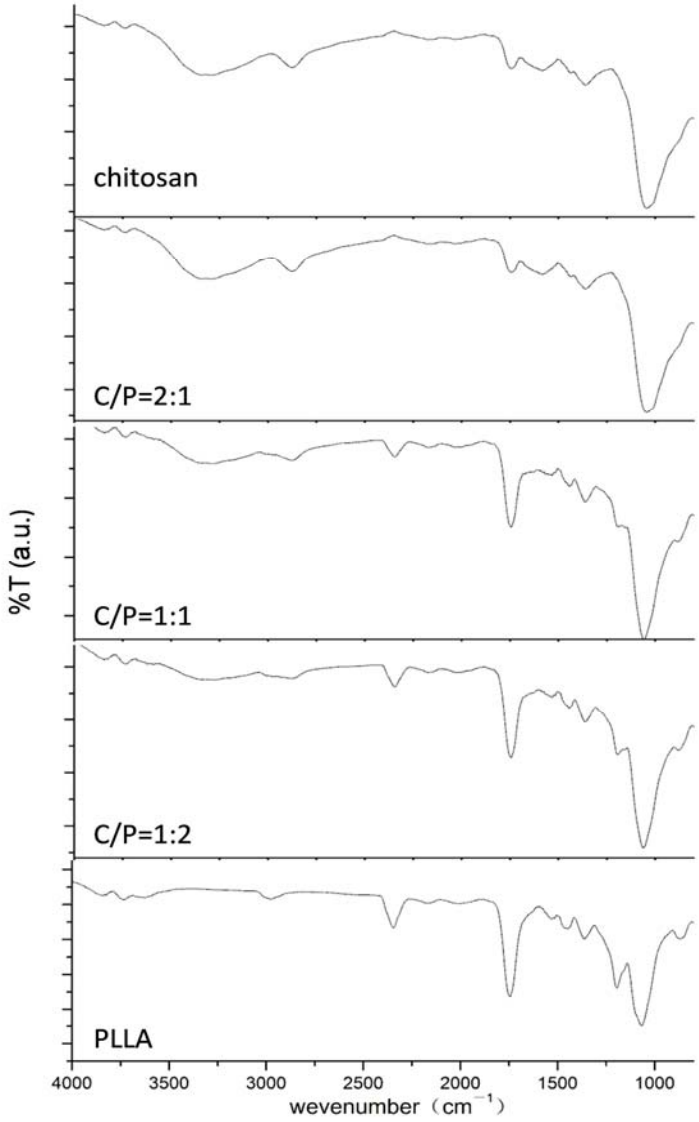

Figure 2. FT-IR spectra of scaffolds.

Kim et al. reported that the hydrophilicity of the material surface could affect its biocompatibility [8]. Chitosan is basically regarded as a hydrophilic biomaterial in biomedical applications. The water contact angle results shown in Table 1 demonstrate that the PLLA scaffolds created have the smallest contact angle. With increased chitosan content, the hydrophilicity of the blended fibrous scaffolds improved and the contact angles increased. The water contact angles of CS/PLLA = 2:1 and neat chitosan could not be measured, as the water was absorbed by the scaffolds. Water uptake results shown in Table 1 suggested that scaffolds from neat CS and CS/PLLA (2:1 and 1:1, respectively) increased to twice the weight of neat PLLA and CS/PLLA (1:2). Water uptake results were consistent with that of water contact angle tests, showing that increased chitosan content improves hydrophilicity of scaffold.

Table 1. Water contact angle and water uptake of fibrous scaffolds

Samples	**Chitosan**	**C/P 2:1**	**C/P 1:1**	**C/P 1:2**	**PLLA**
Contact angle (°)	N/A	N/A	28.2±1.0	64.0±0.5	82.7±0.5
Water uptake (× 100%)	42±3	38±3	32±1	18±3	16±2

The mechanical properties of scaffolds are important in determining its performance. A comparison of the curves in Figure 3 suggests that the incorporation of chitosan into the scaffolds leads to a significant decrease in the tensile strength and ultimate strain. This phenomenon is possibly due to the weak physical properties of chitosan.

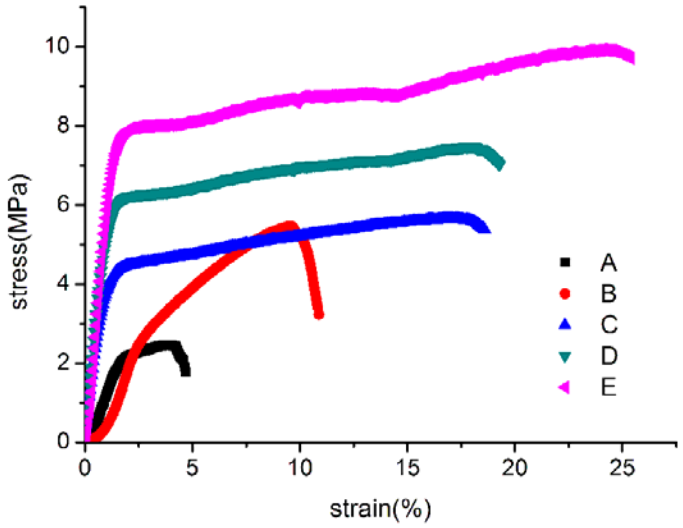

Figure 3. Typical stress-strain curves of each scaffold: (A) CS; (B) CS/PLLA = 2:1; (C) CS/PLLA = 1:1; (D) CS/PLLA = 2:1; (E) PLLA.

Degradation of the scaffolds was also studied, and Figure 4 shows the weight remaining data for the samples in pH 7.4 lysozyme PBS at 37°C. The presence of lysozyme accelerated weight loss, suggesting a degradation of the chitosan within the scaffolds. After 3 weeks, the weight remaining of the chitosan and CS/PLLA scaffolds in lysozyme were less than 85% of the original scaffolds.

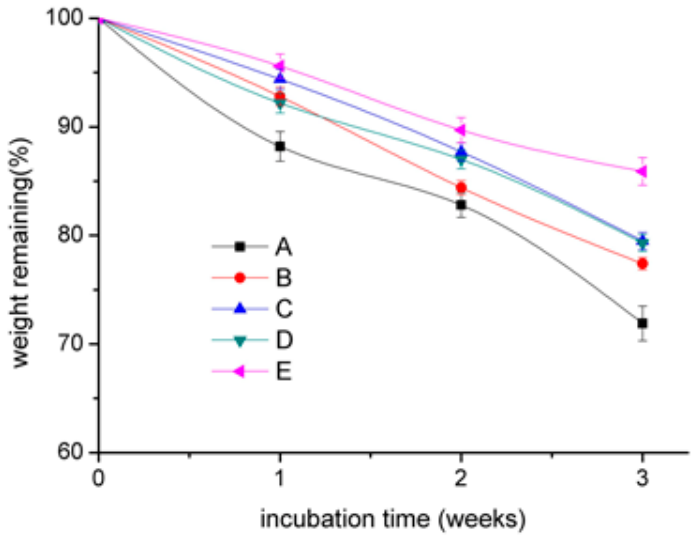

Figure 4. Weight remaining of each scaffold after incubation in lysozyme (0.05wt%) phosphate-buffered solution: (A) CS; (B) CS/PLLA = 2:1; (C) CS/PLLA = 1:1; (D) CS/PLLA = 2:1; (E) PLLA.

The nano/micro-fibrous scaffolds were used to mimic the fibrous morphology of collagen, a major component of bone ECM known to affect osteoblast-like behavior [23]. To study cell adhesion and proliferation on CS/PLLA scaffolds, two-dimensional (2D) TCD was employed as a control; neat PLLA and neat chitosan scaffolds were employed as reference materials. The clonal mouse osteoblastic-like MC3T3-E1 cell line was selected for this study due to its high level of differentiation and its ability to form a well-mineralized bone-like ECM containing osteoblastic differentiation markers, such as alkaline phosphatase (ALP). MC3T3-E1 is an excellent model for differentiation that has a distinct reproducibility advantage over primary cell culture systems. Figure 5 shows the result of the cell adhesion ratio tests. After 3 hours' incubation, 87.5% cells had adhered to the PLLA scaffold, while cell adhesion ratios of the scaffolds composed of CS/PLLA blends were as high as 90%. After 24 hours, the cell adhesion of all scaffolds reached as high as 100%.

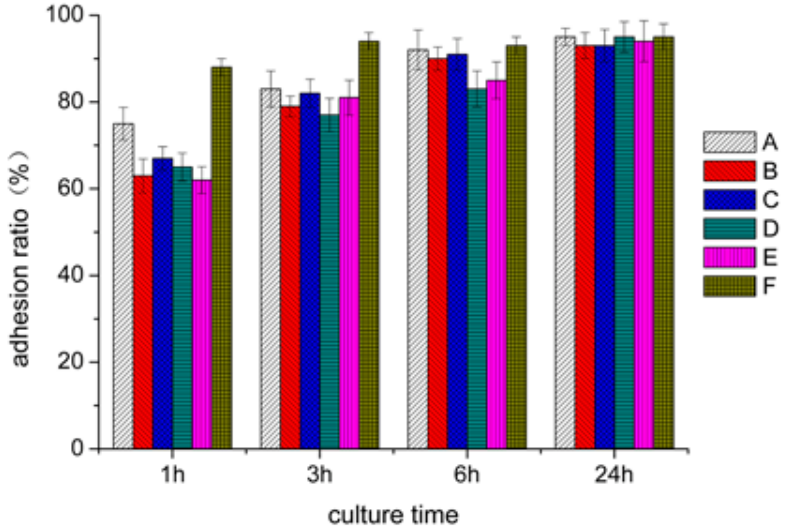

Figure 5. Cell adhesion ratio of MC3T3-E1 cells on each scaffold: (A) CS; (B) CS/PLLA = 2:1; (C) CS/PLLA = 1:1; (D) CS/PLLA = 2:1; (E) PLLA; (F) TCD.

Figure 6 shows the results of cell proliferation assays. Cells cultured on TCD proliferated monotonously and achieved confluence after 5 days of culture. After 14 days' cultivation, the number of cells on CS and CS/PLLA scaffolds were comparable to that on TCD. Nevertheless, neat PLLA scaffolds showed low proliferation activity, even after 21 days' cultivation. During the initial phases, fewer cells proliferated on the fibrous scaffolds than on the TCD control. This can be attributed to the permeability of the porous scaffold, which provides an interconnected structure for cell penetration, while also allowing some cells to attach to the underlying dish. These cells cannot be distinguished by the Tetra Color One method. The cells proliferated similar on all substrates after 14 days, indicating that 3D structure of the fibrous scaffolds facilitated higher cell densities than 2D TCD.

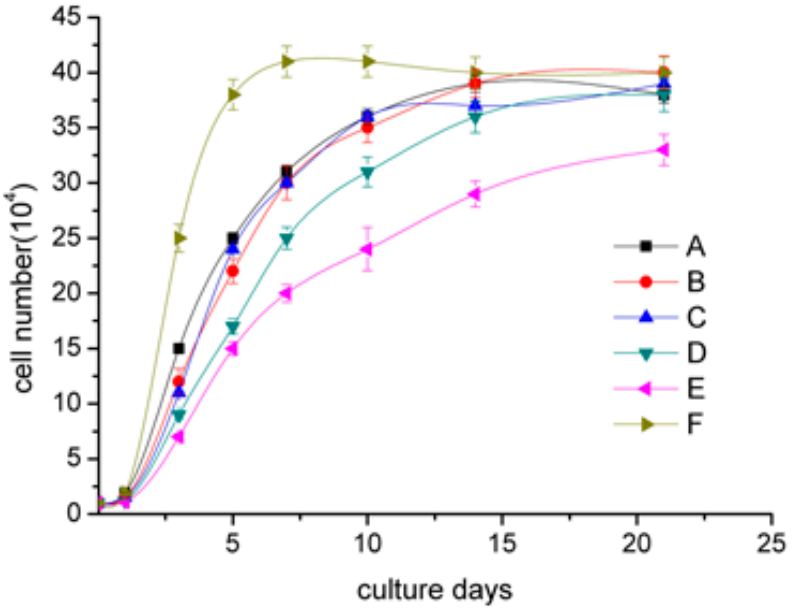

Figure 6. Proliferation of MC3T3-E1 cells on each scaffold: (A) CS; (B) CS/PLLA = 2:1; (C) CS/PLLA = 1:1; (D) CS/PLLA = 2:1; (E) PLLA; (F) TCD.

To investigate the spatial distribution of focal adhesion contacts and the organization of the cytoskeleton, cells were fluorescently stained to visualize vinculin and the nucleus (Figure 7). After 3 days' cultivation, the cell density of the PLLA scaffold (E) was significantly lower than the other scaffolds, which is consistent with the proliferation results. Moreover, cells on the PLLA scaffolds displayed a fusiform morphology, indicating that the cells were confined to a single fiber and aligned along the length of it. This is possibly due to cells being unable to stretch across fibers that are far apart from one another.

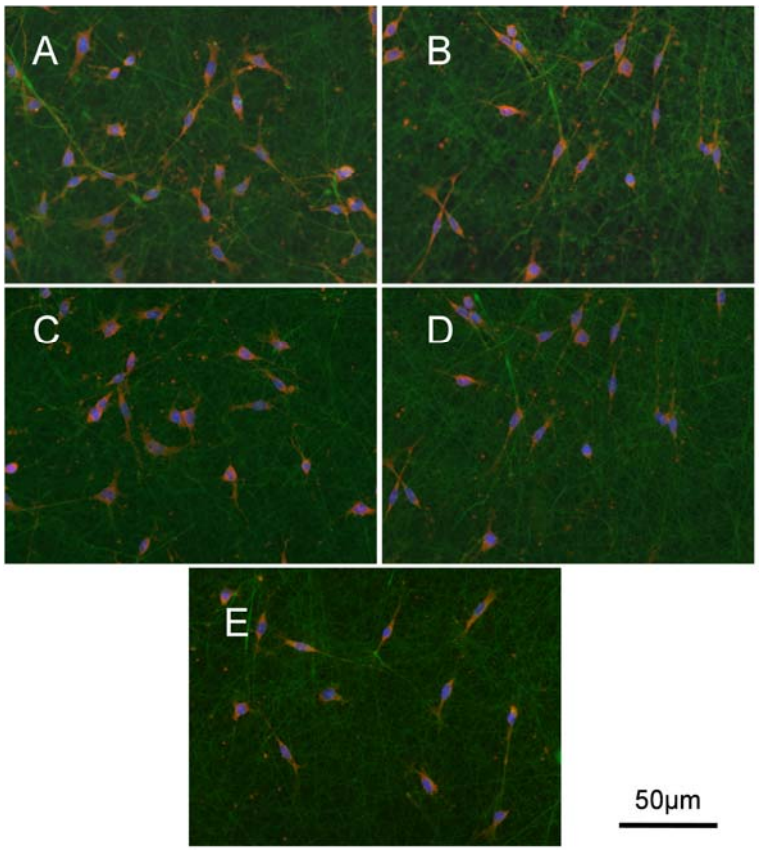

Figure 7. CLSM images of immunohistochemical-stained MC3T3-E1 cells on each scaffold. Fluorescent staining of fiber (green), vinculin (red), and cell nuclei (blue): (A) CS; (B) CS/PLLA = 2:1; (C) CS/PLLA = 1:1; (D) CS/PLLA = 2:1; (E) PLLA.

Conversely, cells on CS/PLLA and CS scaffolds showed both fusiform and polygonal morphology. The biological superiority of the scaffolds incorporating chitosan in the electrospun fibers is demonstrated by the improvement of osteoblast-like adhesion and rapid spreading. This was most likely due to chitosan having better cell compatibility than PLLA, thereby being more beneficial for cell migration.

Early-phase cell differentiation activity, as monitored by ALP activity, was positively impacted by cell interactions with the 3D scaffolds. The results in Figure 8 show that cells cultured on TCD had the

lowest ALP activity. With an increase in CS content, scaffolds showed higher ALP activities. Cells on neat CS showed the highest ALP activity. Since all of the fibrous scaffolds were essentially similar in structure, the greater ALP activities at early phase differentiation on CS and CS/PLLA scaffolds indicate that chitosan may provide MC3T3-E1 cells with a more robust foundation to commence differentiation.

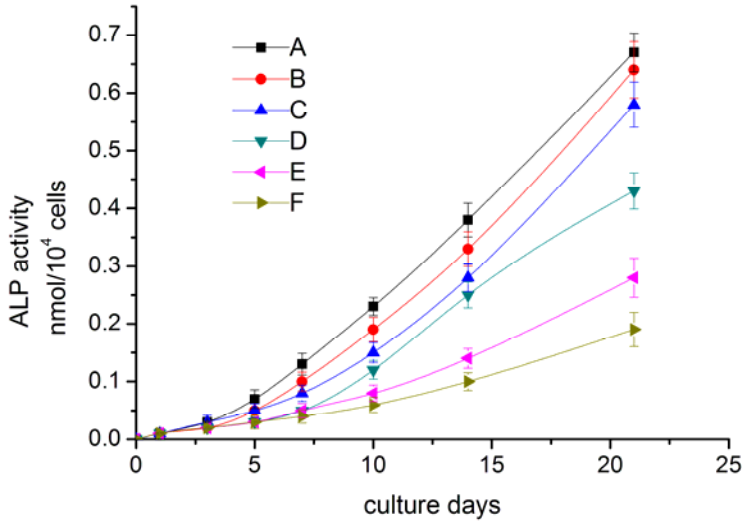

Figure 8. ALP activity of MC3T3-E1 cells on each scaffold: (A) CS; (B) CS/PLLA = 2:1; (C) CS/PLLA = 1:1; (D) CS/PLLA = 2:1; (E) PLLA; (F) TCD.

The ALP kinetics results of this study are consistent with previous publication. The enzymatic activity significantly increases on the fibrous scaffolds following proliferation, in comparison to TCD. Furthermore, the ALP activity profile for cells on CS and CS/PLLA scaffolds, which coincides with the mineralization process, was typical of the enzyme expression that occurs in the early stages of differentiation [26].

In the final stage of osteoblast-like maturation, ECM mineralization of the differentiated cells was measured through calcium deposition. Figure 9 shows calcium deposition results of MC3T3-E1 cultured on the

scaffolds. Cells cultured on TCD show low calcium deposition. With the increase of CS content, scaffolds show higher calcium deposition. Cells on neat CS have the highest calcium deposition.

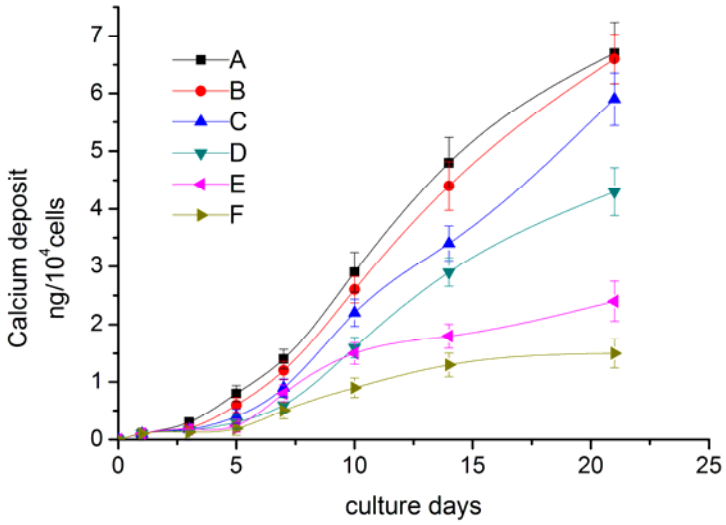

Figure 9. Calcium deposition of MC3T3-E1 cells on each scaffold: (A) CS; (B) CS/PLLA = 2:1; (C) CS/PLLA = 1:1; (D) CS/PLLA = 2:1; (E) PLLA; (F) TCD.

Based on these results, the osteoblast-like host response to fibrous substitutes significantly varied with chitosan content. Cells on CS/PLLA = 2:1 and 1:1 scaffolds had almost identical bioactivities, whereas CS/PLLA = 1:2 (lower chitosan content) had decreased biocompatibility, suggesting that a more optimal ratio of chitosan to PLLA could improve MC3T3-E1 cell adhesion to the CS/PLLA composite scaffolds. This is owing to the fact that when materials are exposed to dilute serum, hydrophilic surfaces are more effective than hydrophobic surfaces for cell attachment, spreading, and cytoskeletal organization [17, 28]. Moreover, chitosan can enhance the formation of new bone tissue by increasing osseointegration expression and the deposition of calcium minerals on its surface. Several studies have illustrated that the cationic

nature of chitosan allows for electrostatic interactions with anionic GAGs, PGAs, and other negatively-charged materials [19, 25, 26]. These ionic interactions may serve as a mechanism for retaining and recruiting cells, growth factors, and cytokines within a tissue engineering scaffold.

Although neat chitosan can be electrospun into nano/micro-fibers, which have been shown to be more favorable for cell attachment, its rapid degradation can lead to mechanical instability. The composite CS/PLLA nanofibers are considered more effective at mimicking native ECM, in both topology and composition, with improved mechanical stability.

4. Conclusion

CS/PLLA-blend nano/micro-scaffolds, with porous 3D architecture, were successfully prepared by electrospinning. The FT-IR results show that there were no reactions between the two materials, suggesting that blend spinning maintained the bioactive amino group of chitosan. Due to the high mechanical strength of PLLA, the tensile properties of CS/PLLA scaffolds increased with a corresponding increase in PLLA content. Nevertheless, the high PLLA content in the blends resulted in a slowing of the degradation rate. Cell experiment results show that an increased weight percentage of chitosan is effective in enhancing cell adhesion, proliferation, and mineralization. Therefore, the results suggest that the increased hydrophilicity of the material surface could improve its biocompatibility. CS/PLLA = 1:1 and 2:1 scaffolds were found to exhibit the most effective physicochemical and osteoconductive characteristics, with a good potential for application in bone tissue engineering.

Acknowledgement

This work was supported by Grant-in-Aid for Global COE program by the Ministry of Education, Culture, Sports, Science, and Technology.

Reference

[1] Narayan Bhattarai, Dennies Edmondson and Omid Veiseh et al., Electrospun chitosan-based nanofibers and their cellular compatibility, Biomaterials 26(7) (2005), 6176-6184.

[2] Cheng Chen, Lisong Dong and Man Ken Cheung, Preparation and characterization of biodegradable poly(L-lactide)/chitosan blends, European Polymer Journal 41 (2005), 958-966.

[3] Victor J. Chen, Laura A. Smith and Peter X. Ma, Bone regeneration on computer-designed nano-fibrous scaffolds, Biomaterials 27(21) (2006), 3973-3979.

[4] Catherine M. Cowan, Chia Soo, Kang Ting and Benjamin Wu, Evolving concepts in bone tissue engineering, Current Topics in Developmental Biology 66 (2005), 239-285.

[5] Yuan Lu Cui and Xin Hou, Biomimetic surface modification of ploy(L-lactic acid) with gelatin and its effects on auricular chondrocytes in vitro, Biomaterials 24(7) (2003), 3859-3868.

[6] Zhi Ding, Jiangning Chen, Shuying Gao, Jianbing Chang, Junfeng Zhang and E. T. Kang, Immobilization of chitosan onto poly-lactic acid film surface by plasma graft polymerization to control the morphology of fibroblast and liver cells, Biomaterials 25(6) (2004), 1059-1067.

[7] Dietmar W. Hutmacher, Scaffolds in tissue engineering bone and cartilage, Biomaterials 21(4) (2000), 2529-2543.

[8] K. Kim, M. Yu, X. Zong, J. Chiu, D. Fang and Y. S. Seo, Control of degradation rate and hydrophilicity in electrospun non-woven poly(D, L-lactide) nanofiber scaffolds for biomedical applications, Biomaterials 24(27) (2003), 4977-4985.

[9] Áron Lazáry, Bernadett Balla, János P. Kósa, Krisztián Bácsi, Zsolt Nagy, István Takács, Péter P. Varga, Gábor Speer and Péter Lakatos, Effect of gypsum on proliferation and differentiation of MC3T3-E1 mouse osteoblastic cells, Biomaterials 28(3) (2001), 393-399.

[10] Soo-Hong Lee and Heungsoo Shin, Matrices and scaffolds for delivery of bioactive molecules in bone and cartilage tissue engineering, Advanced Drug Delivery Reviews 59(4-5) (2007), 339-359.

[11] W. J. Li, C. T. Laurencin, E. J. Caterson, R. S. Tuan and F. K. Ko, Electrospun nano-fibrous structure: A novel scaffold for tissue engineering, J. Biomed. Mater. Res. 60(4) (2002), 613-621.

[12] Wen Liang, Mohamed N. Rahaman, Delbert E. Day, Nicholas W. Marion, Gwendolen C. Riley and Jeremy J. Mao, Bioactive borate glass scaffold for bone tissue engineering, Journal of Non-Crystalline Solids 354(15-16) (2008), 1690-1696.

[13] Ying Luo, George Engelmayr, Debra T. Auguste, Lino da Silva Ferreira, M. Karp Jeffrey, Rajiv Saigal and Robert Langer, Three-dimensional scaffolds, Principles of Tissue Engineering (Third Edition) (2007), 359-373.

[14] João F. Mano, Graham Hungerford and José L. Gómez Ribelles, Bioactive poly(L-lactic acid)-chitosan hybrid scaffolds, Materials Science and Engineering C 28(8) (2008), 1356-1365.

[15] R. A. A. Muzzarelli, C. Jeuniaux and G. W. Gooday, Chitin in Nature and Technology, Plenum, New York, 1986.

[16] Karthikeyan Narayanan, Kwong-Joo Leck, Shujun Gao and Andrew C. A. Wan, Three-dimensional reconstituted extracellular matrix scaffolds for tissue engineering, Biomaterials 30(26) (2009), 4309-4317.

[17] D. L. Nettles, S. H. Elder and J. A. Gilbert, Potential use of chitosan as a cell scaffold material for cartilage tissue engineering, Tissue Eng. 8 (2002), 1009-1016.

[18] Kousaku Ohkawa et al., Electrospinning of chitosan, Macromol. Rapid Commun. 25 (2004), 1600-1605.

[19] T. A. Owen and M. Aronow et al., Progressive development of the rat osteoblast phenotype in vitro: Reciprocal relationships in expression of genes associated with osteoblast proliferation and differentiation during formation of the bone extracellular matrix, J. Cell Physiol. (1990), 143.

[20] K. Rezwan, Q. Z. Chen, J. J. Blaker and Aldo Roberto Boccaccini, Biodegradable and bioactive porous polymer/inorganic composite scaffolds for bone tissue engineering, Biomaterials 27(18) (2006), 3413-3431.

[21] J. H. G. Rocha, A. F. Lemos, S. Agathopoulos, P. Valério, S. Kannan, F. N. Oktar and J. M. F. Ferreira, Scaffolds for bone restoration from cuttlefish, Bone 37(6) (2005), 850-857.

[22] Patricia M. Taylora, Anthony E. G. Cass and Magdi H. Yacoub, Extracellular matrix scaffolds for tissue engineering heart valves, Progress in Pediatric Cardiology 21(2) (2006), 219-225.

[23] K. Webb, V. Hlady and P. A. Tresco, Relative importance of surface wettability and charged functional groups on NIH3T3 fibroblast attachment, spreading, and cytoskeletal organization, J. Biomed. Mater. Res. 41 (1998), 422-430.

[24] Chengtie Wu, Yogambha Ramaswamy, Philip Boughton and Hala Zreiqat, Improvement of mechanical and biological properties of porous $CaSiO_3$ scaffolds by poly(d,l-lactic acid) modification, Acta Biomaterialia 4(2) (2008), 343-353.

[25] Hua Wu, Ying Wan, Xiaoying Cao and Quan Wu, Proliferation of chondrocytes on porous poly(d, l-lactide)/chitosan scaffolds, Acta Biomaterialia 4(1) (2008), 76-87.

[26] Shintaro Yamanen, Norimasa Iwasakia, Tokifumi Majima, Tadanao Funakoshia, Tatsuya Masuko, Kazuo Harada, Akio Minami, Kenji Monde and Shin-Ichiro Nishimura, Feasibility of chitosan-based hyaluronic acid hybrid biomaterial for a novel scaffold in cartilage tissue engineering, Biomaterials 26(6) (2005), 611-619.

[27] F. Yang, R. Murugan, S. Wang and S. Ramakrishna, Electrospinning of nano/micro scale poly(L-lactic acid) aligned fibers and their potential in neural tissue engineering, Biomaterials 26(15) (2005), 2603-2610.

[28] Xiufang Zhang, Hui Hua, Xinyuan Shen and Qing Yang, In vitro degradation and biocompatibility of poly(L-lactic acid)/chitosan fiber composites, Polymer 48 (2007), 1005-1011.

■